Gamma Radiation Tests of Potential Optical Fiber Candidates for Fibroscopy

O. Deparis [1,2], P. Mégret [2], M. Decréton [1], M. Blondel [2]

[1] SCK•CEN, Nuclear Research Center, 200 Boeretang, B-2400 Mol
[2] Faculté Polytechnique de Mons, 31 boulevard Dolez, B-7000 Mons

Abstract

Two pure silica core F-doped silica cladding multimode step-index (MMSI) fibers were selected and exposed to γ rays up to 1.5 MGy. One is a conventional polyimide coated high OH fiber (Suprasil® F-100 core material). The other is a new type of low OH low Cl aluminium coated fiber whose core material is made of KS-4V glass. Two successive irradiations, separated by a 3-days recovery time, were performed at 4.9 kGy/h and 60 °C. Radiation-induced attenuation spectra were recorded *in situ* from 400 nm to 1200 nm using a white light source and an Optical Spectrum Analyser. In the conventional fiber, the induced attenuation spectra were governed by the growth and the recovery of the 600 nm band associated to Non-Bridging Oxygen Hole Centers (NBOHCs). By contrast, for doses higher than 100 kGy, the KS-4V fiber showed fairly dose and time-invariant spectra (attenuation values of few dB/m decrease with increasing wavelength in the visible range). Because of the absence of the 600 nm band, the KS-4V fiber, beside the conventional fiber, appears to be a very promising candidate for fibroscopy.

I. INTRODUCTION

Besides the application field of infrared data transmission, the optical fibers offer by means of fibroscopy the possibility of visual inspection in nuclear power plants and monitoring of radioactive waste disposal sites [1]. However light transmission in optical fibers exposed to radiations is much more degraded in the visible than in the infrared [1] [2] [3] [4]. In the visible range (400-700 nm), the radiation-induced attenuation mainly results from the superposition of a band tail extending from the ultraviolet and a band near 600 nm [4] [5]. The former (called "UV band tail") is attributed to chlorine impurities and/or intrinsic color centers and the latter to the nonbridging oxygen hole center [4] [5]. A 660 nm band (decreasing above ≈2 kGy) has also been observed in low OH silicas [4] [6]. For conventional fibers manufactured from $SiCl_4$ raw material, the better radiation resistance of high OH fibers is related to their low Cl content in the core [6]. Low OH and low Cl contents minimize the concentration of Non-bridging Oxygen Hole Centers (NBOHCs) responsible for the 600 nm band and the UV band tail, respectively. However, reducing *both* Cl and OH contents simultaneously is unachievable with the conventional technology [5]. Using another glass fabrication technology ("KS-4V glass" [5]), it is now possible to produce extremely pure synthetic silica with both low OH and Cl contents. Moreover high temperature heating of the fiber during the application of an aluminium coating anneals structural defects such as NBOHCs [5].

An *ideal* fibroscope should meet, at least, two requirements in the visible range : low absolute level of radiation induced attenuation and flat spectrum. Together, these two requirements ensure a transmission of the light with minimal attenuation and no spectral distortion of the colors.

In this paper we present gamma radiation test results on two optical fiber potential candidates for fibroscopy : one is manufactured from KS-4V glass and the other from $SiCl_4$. The latter was chosen for its good gamma radiation and high temperature resistance among four other $SiCl_4$-based fibers also tested but not discussed here.

II. EXPERIMENTAL

The main characteristics of the two potential candidates we selected for fibroscopy are shown in Table 1. Both are multimode step-index (MMSI) fibers having pure silica core and fluorine-doped cladding applied by Plasma Outside Deposition process. The fiber A is a conventional high OH fiber drawn from a Fluosil® preform (core material Suprasil® F-100). It has a small core/cladding diameter ratio (1.1) and a polyimide coating. Because of its high OH and low Cl contents, this fiber is known to have a better radiation resistance compared to a conventional low OH fiber (Suprasil® F-300) [3] [4]. The fiber B is a new type of fiber [5]. It was manufactured on the basis of KS-4V glass without using $SiCl_4$ as raw material [5]. It has both low OH and low Cl contents and an aluminium coating.

Table 1

Potential candidates selected from irradiation test results

Fiber	A	B
Technology	$SiCl_4$ based	KS-4V glass
Diam. (μm)	100/110/125	100/120/150
Coating	polyimide	aluminium
[OH] (ppm)	600-800	< 0.2
[Cl] (ppm)	100-125	< 20

The irradiation tests were performed in the gamma facility of SCK•CEN, Mol, Belgium [3]. A heating system allowed to

0018-9499/96$05.00

keep a stable temperature of 60 °C. A lower value would result in temperature fluctuations caused by gamma heating. Moreover, this test temperature is typical of the ambient temperature encountered during in-vessel maintenance of a Fusion reactor. Only for a few hours during recovery periods, the temperature was raised to 80 °C (or 75 °C) or was lowered to 40 °C. The dose rate was measured at 9 levels using Perpex dosimeters [3]. The irradiation was performed in several steps at a dose rate of 4.9 kGy(SiO_2)/h. The fibers were first irradiated up to 0.8 MGy(SiO_2) and then taken out of the facility for a 3 days recovery period (Cycle I). This sequence could happen when the fibroscope is exposed to γ radiations for its very first task or when it is intentionally pre-irradiated for hardening purposes [4]. A second irradiation took place at the same dose rate to reach the total dose of 1.5 MGy(SiO_2) followed by a 9 days recovery period (Cycle II). The sample length exposed to radiations was wound on a 54 mm diameter spool, made of aluminium. The spool height was small enough (56 mm) to assume uniformity of the gamma flux on the sample length which is 10 m for fiber A and 6 m for fiber B. The two 20 m pigtail extensions of each coil were led out the facility and spliced to a fiber-based switching system.

The radiation-induced attenuation is measured *in situ* from 400 nm to 1400 nm (steps of 10 nm) and computed following ref. [3] as recommended by the ASTM Standard Guide [7]. The experimental set-up is shown at fig. 1.

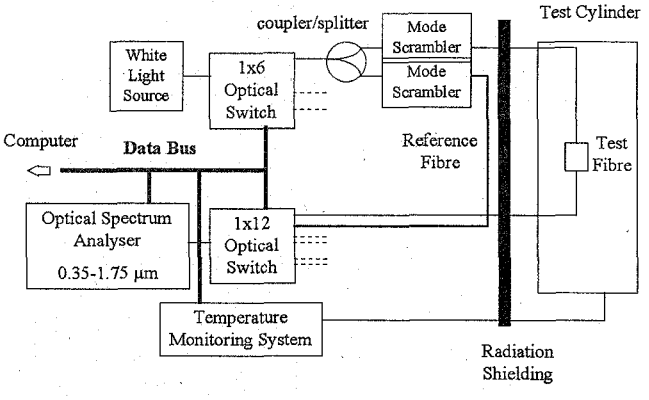

Fig. 1 : The experimental set-up for measuring the radiation-induced spectral attenuation (following ASTM Standard Guide [7]).

A Tungsten-Halogen source injects the light into both the irradiated fiber and the unirradiated reference fiber by means of an optical coupler/splitter and a mode scrambler. Light is not injected between two measurements, except for some intermediate periods during irradiations (20 min per hour of illumination during these periods). In the visible range, the light level emitted by the source inevitably decreases with decreasing wavelength. If photobleaching takes place in the fibers, it might be less efficient in the lower part of the visible spectrum. At the output of fiber A, the light level (10 nm bandpass) is -62.0 dBm at 400 nm and -48.0 dBm at 700 nm. These values were 4 dB lower for the fiber B due to higher bending losses. The output light spectra are sequentially measured by an Optical Spectrum Analyser. The fiber-based switching system selects the fiber to be measured. Note that a small length of each pigtails (only 600 mm) is exposed the non-uniform gamma flux. This constraint limits the accuracy of the measurement expressed in dB per meter. Induced attenuation in these lengths could be cancelled by also exposing a short length of the reference fiber to radiations [8].

III. RESULTS

The spectra of the radiation induced attenuation are shown in fig. 2 for the fiber A during the first cycle. Because of the intense first OH overtone band near 950 nm and high bending losses, the induced-attenuation was not measurable around 950 nm and above ≈1200 nm, respectively.

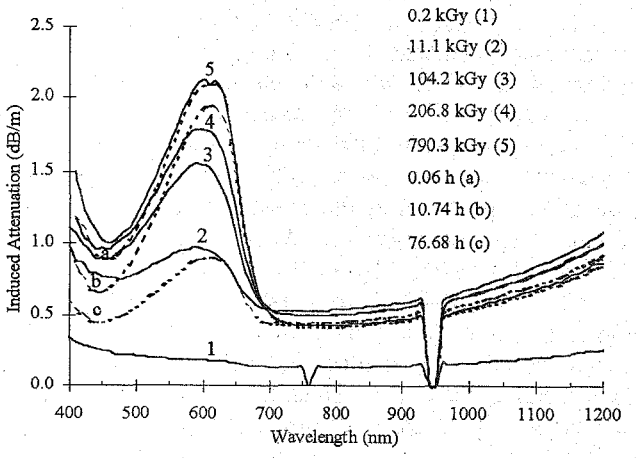

Fig. 2: Induced attenuation spectra in fiber A during the first cycle. The legends (1-5) give the dose (kGy(SiO_2)) absorbed during irradiation. The legends (a-c) give the recovery time since the end of this first irradiation (hours).

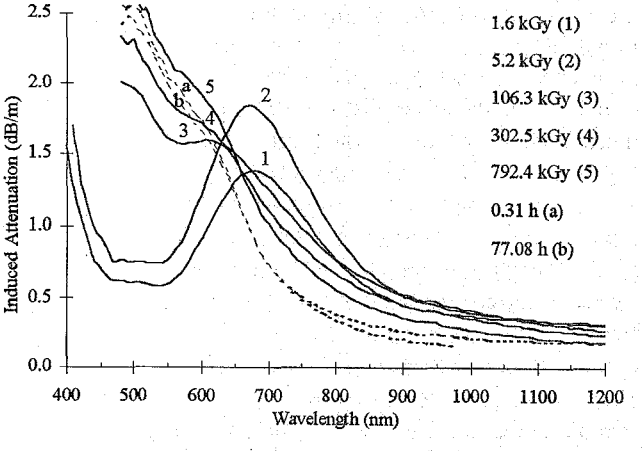

Fig. 3 : Induced attenuation spectra in fiber B during the first cycle. Legends have the same meaning as those of fig. 2. Note that data below 480 nm are out of the dynamic range and thus not displayed.

During the first irradiation (fig. 2, curves 1-5) a well-defined absorption band around 600 nm grows with dose and then saturates. It is attributed to the Non Bridging Oxygen Hole

Centers (≡Si–O•) for which different formation mechanisms have been suggested [4] [6] [9] depending on the type of precursor (≡Si–O–H, ≡Si–O–O–Si≡). Extending from the ultraviolet to the visible (see data in the 400-500 nm range), a UV band tail also grows and saturates. It is attributed to interstitial atomic chlorine [4]. After irradiation (fig. 2, curves a-c), both the 600 nm band and the UV band tail recover. On the other hand, the spectra of the fiber B reveal a radically different behavior during this first cycle (fig. 3). In the very beginning of the irradiation (fig. 3, curves 1-2), a transient absorption band at 660 nm grows quickly and then decreases for doses > 4.0 kGy. We reported and discussed this 660 nm band in [10]. This band has been previously observed in low OH fibers and attributed to an unidentified impurity [6]. Because the 660 nm band does not appear any more during the second irradiation, one can conclude that it is bleachable by the radiations themselves. A pre-irradiation up to a few kGy could completely eliminate this absorption band. For higher doses and up to the final dose of 0.8 MGy (curves 3-5), the spectrum of the induced attenuation is fairly dose-invariant: attenuation values in the visible decrease with increasing wavelength but a small "shoulder" is observed around 600 nm. This is consistent with previous reported results [5] in which the 600 nm band was found to be practically absent from post irradiation attenuation spectra. This feature was attributed to the annealing of NBOHC precursors during aluminium coating application at high temperature [5]. The chlorine content is very low in KS-4V glass (see Table 1). Thus only intrinsic defects having absorption bands in the UV could explain the origin of the UV band tail in this fiber. After irradiation, the fiber B does not recover much compared to the fiber A.

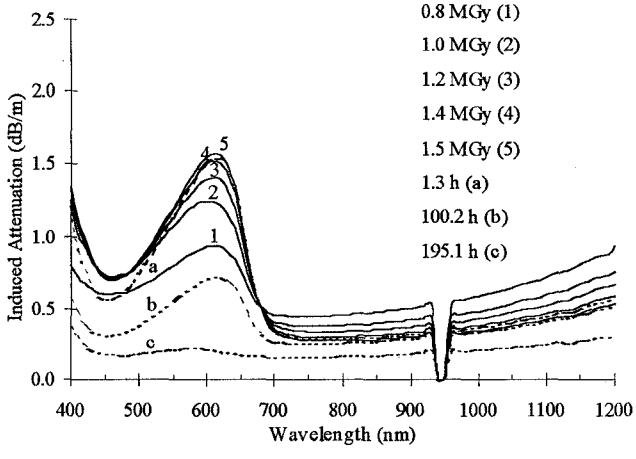

Fig. 4 : Induced attenuation spectra in fiber A during the second cycle. The legends (1-5) give the dose ($MGy(SiO_2)$) cumulated with that achieved at the end of the first irradiation. The legends (a-c) give the recovery time since the end of this second irradiation (hours).

The second cycle confirmed the trends observed in the two fibers during the first cycle. On one hand, the fiber A (fig. 4) still shows a 600 nm band together with a UV band tail, both growing with dose, then saturating (fig. 4, curves 1-5) and recovering after irradiation (fig. 4, curves a-c). Compared to the first irradiation, the saturation of the 600 nm band with increasing dose is stronger. On the other hand, the fiber B (fig. 5) shows a fairly dose or time-invariant induced attenuation spectrum, during irradiation (fig. 5, curves 1-5) or recovery (fig. 5, curves a-b). In this fiber, the intrinsic defects in the UV range limit the ultimate performances.

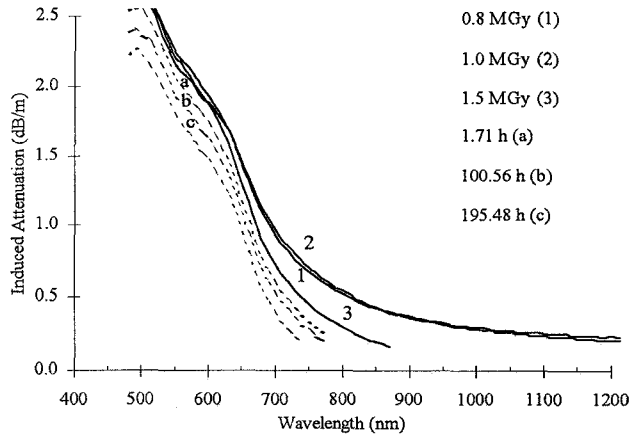

Fig. 5 : Induced attenuation spectra in fiber B during the second cycle. Legends have the same meaning as those of fig. 4.

In order to discuss the performances of the two types of fiber, their radiation-induced attenuation at 600 nm and 850 nm are shown in fig. 6 during the two successive cycles. During the first irradiation (fig. 6, 1st chart), saturation of the induced attenuation at 600 nm takes place in both fibers. The observed difference in kinetics is a consequence of the different physical origins of the induced attenuation (see above, fig. 2 and 3). The evolution of the induced attenuation at 660 nm in fiber B points out the existence of the radiation bleachable absorption band at 660 nm. After this first irradiation, the fiber A recovers significantly at 600 nm while the fiber B much less (fig. 6, 2nd chart). Note that, for both fibers, radiation hardening of the induced attenuation takes place in the infrared [4] during the two irradiations (see fig. 6, 1st and 3rd charts, curves at 850 nm).

Between time values of 25 h and 55 h (e.g. fig. 6, 2nd chart, curves at 850 nm or 600 nm), a temporary heating was performed up to 75°C before returning to 60°C. Surprisingly, at any wavelength, the induced attenuation increases as the temperature rises. Thermal bleaching of color centers can not be put forward to explain this, because it produces the opposite effect [1]. Attenuation and temperature data were strongly correlated here: correlation coefficients of 0.98 and 0.64 were found for fibers A and B respectively (at 850 nm). Such positive values were confirmed by both temporary heating (80°C) and cooling (40°C) performed at the end of the second recovery (not shown on fig. 6). The same phenomenon observed in the four other Polymicro fibers (not discussed here) revealed coating material and cladding thickness dependencies. This phenomenon is due to microbending losses induced by the thermal expansion of the aluminium spools on which the fibers are wound [11].

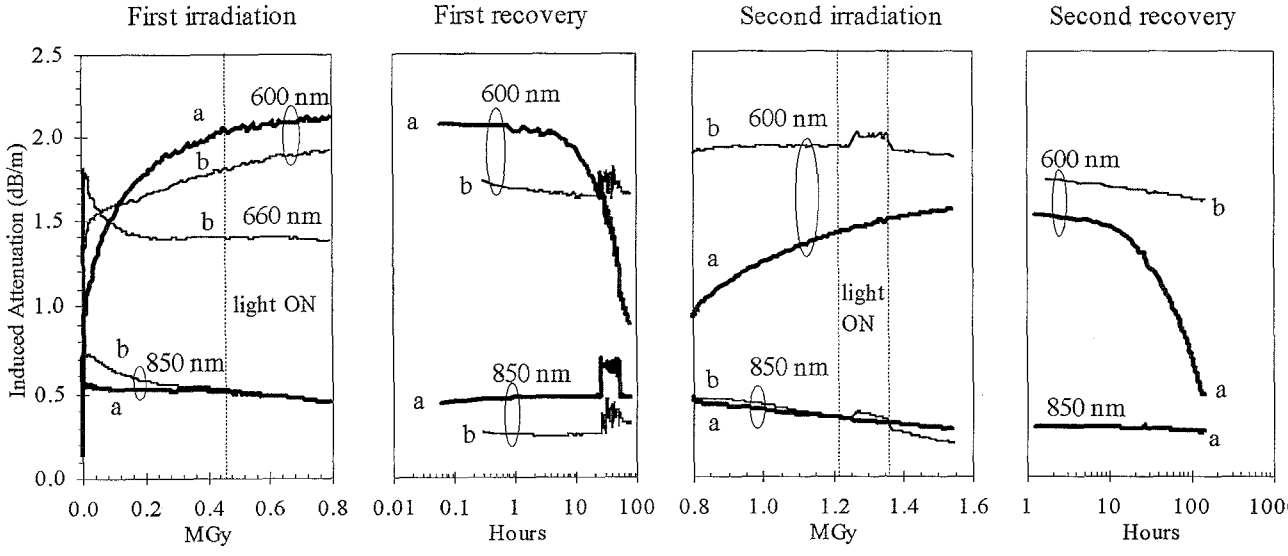

Fig. 6 : Evolution of the induced attenuation at 600 nm and 850 nm during the two irradiation and recovery cycles for fiber A (a) (thick lines) and fiber B (b) (thin lines) fibers. During the first irradiation, induced attenuation at 660 nm is displayed for fiber B. During the last recovery, induced attenuation at 850 nm is zero for fiber B and thus not displayed. During intermediate periods (1st and 2nd irradiations) light was injected between two measurements (light ON 20min. per hour).

Moreover, microbending losses are induced, from the start, by raising the temperature from 20 °C, at which the fiber were wound and measured *before* irradiation, to 60 °C where the irradiation-recovery cycles were performed.

Finally, we can note that no photobleaching effect [4], i.e. photostimulated annealing of color centers, is observable during the period of illumination (fig. 6, 1st irradiation with "light ON").

In the visible range, the distinction between the two fibers is clear during the second cycle (fig. 6, 3rd and 4th charts, curves at 600 nm). Compared to the first cycle, the fiber A behaves similarly : the induced attenuation grows, saturates and recovers following the evolution of NBOHC-related band. However the stronger saturation reveals a hardening effect [3] due to the first irradiation. This points out the capability of a pre-irradiation to improve the fiber response [3]. In the case of fiber B, the fluctuations of attenuation values between 1.25 MGy and 1.35 MGy are due to a drastic diminution (6 dB) of injected light level caused by a wrong replacement of the Tungsten-Halogen lamp after break down. It is fortuitous that this artefact happens during the intermediate period of illumination (fig. 6, 2nd irradiation with "light ON"). We can thus also conclude that no photobleaching occurs in both fibers. Moreover, the induced attenuation in fiber B does not grow any more during the second irradiation. A radiation hardening is even initiated for doses higher than $\approx$ 1.4 MGy (if we exclude the data recorded during the artefact). Therefore, extrapolation of the fiber response to higher doses (> 1.5 MGy) is, to some extent, possible. After this second irradiation, the fiber B slightly recovers compared to the fiber A.

IV. CONCLUSIONS

For the fiber B, except a 660 nm band observed during the very beginning of first irradiation, the induced attenuation spectrum is always fairly dose-invariant. It slowly decreases with increasing wavelength both in the visible (400-700 nm) and the infrared. Moreover we found that the 660 nm band was bleachable by the radiations : a pre-irradiation of a few kGy is sufficient to eliminate it definitively. The induced attenuation at 600 nm (typical) grows and saturates with dose during the first irradiation but does not recover much after irradiation. During the second irradiation, it does not grow any more with dose (showing even a radiation hardening for doses >1.4 MGy) and slightly recovers after irradiation.

For the fiber A, the radiation response is radically different. In the visible, the induced attenuation spectrum is mainly governed by the dose or time-varying 600 nm absorption band attributed to NBOHCs. The induced attenuation at 600 nm grows and saturates with dose during the first irradiation and recovers significantly after irradiation. During the second cycle, a similar behavior is observed but the stronger saturation reveals a hardening effect due to the first irradiation.

For a fibroscopic application, both fibers meet the first requirement, i.e. a low absolute level of radiation-induced attenuation. With the fiber B, provided a pre-irradiation is performed, the transmission of the light is stable with respect to dose or time (however short wavelengths will experience more attenuation than long wavelengths). To some extent, extrapolation of this behavior to higher doses (> 1.5 MGy) is allowed. By contrast, due to its induced absorption band at 600 nm, the fiber A shows a dose or time-variant induced

attenuation spectrum during both irradiation and recovery cycles. Because of the absence of the 600 nm band, the low OH low Cl aluminium coated fiber, beside the conventionnal high OH fiber, appears to be a very promising candidate for fibroscopy. However, improvement of the fiber response in the near ultraviolet range is needed to meet the second *ideal* requirement for fibroscopy : a *flat* (i.e wavelength independent) induced attenuation spectrum.

V. ACKNOWLEDGEMENTS

The authors gratefully acknowledge Dr K. M. Golant from the Fiber Optic Research Center (Moscow) who supplied the fiber B and Dr D. L. Griscom (Naval Research Laboratory, Washington) for instructive discussions about this study. They also thank F. Vos and C. Van Ierschot (SCK•CEN) for their technical support during the irradiation tests.

VI. REFERENCES

[1] F. Berghmans, O. Deparis, S. Coenen, M. Decréton, P. Jucker, "Optical Fibres in Nuclear Radiation Environments ", in *Trends in Optical Fibre Metrology and Standards,* NATO ASI Series (E), vol. 285, Olivério. D. D. Soares, Ed., Dordrecht-Boston-London : Kluwer Academic Publishers, 1995, pp. 131-156.

[2] E. W. Taylor, E. J. Friebele, H. Henschel, R. H. West, J. A. Krinsky, C. E. Barnes, "Interlaboratory Comparison of Radiation-Induced Attenuation in Optical Fibers. Part II : Steady-State Exposures", *J. Lightwave Tech.*, vol. 8, (n° 6), pp. 967-976, 1990.

[3] O. Deparis, P. Mégret, M. Decréton, M. Blondel, "The Radiation-Induced Absorption Band at 600 nm and its Impact in Fibroscopy", in *Proc. RADECS'95*, pp. 507-511, 1995.

[4] D. L. Griscom, "Radiation Hardening of Pure-Silica-Core Optical Fibers by Ultra-High-Dose γ-Ray Preirradiation", in *Proc. RADECS'95*, pp.498-502, 1995.

[5] V.A. Bogatyrjov, I. I. Cheremisin, E. M. Dianov, K. M. Golant, A. L. Tomashuk, "Super High Strength Metal Coated Low Hydroxyl Low Chlorine All Silica Optical Fibres", in *Proc. RADECS'95*, pp. 53-506, 1995.

[6] K. Nagasawa, M. Tanabe, K. Yahagi, "Gamma-Ray-Induced Absorption Bands in Pure-Silica-Core Fibers", *Japanese. J. Appl. Phys.*, vol. 23 , (n°12), pp. 1608-1613, 1984.

[7] Standard Guide E 1614-94, American Society for Testing and Materials, 1994.

[8] D. L. Griscom, "Fast-neutron radiation effects in a silica-core optical fiber studied by a CCD-camera spectrometer ", *J. Appl. Optics,* vol. 33, (n°6), pp.1022 - 1028, 1994.

[9] S. Munekuni,T. Yamanaka, Y. Shimogaichi, R. Thomon, Y. Ohki, K. Nagasawa, Y. Hama, "Various type of non bridging oxygen hole center in high-purity glass ", *J. Appl. Phys.*, vol. 68, (n°3), pp.1212-1217, 1990.

[10] O. Deparis, P. Mégret, M. Decréton, M. Blondel, "Evolution of the 660 nm Radiation-Induced Band in a Low-OH Low-Cl Optical Fibre"; *IEE Electronics Letters*, vol. 32, (n°15), pp. 1392-93, July 1996.

[11] This explanation has been confirmed by the following experiment. We performed thermal tests (heating from room temperature to 100°C) on fiber samples similar to those discussed in this study but having *never been irradiated.* These samples were wound on aluminium spools of 54 mm diameter. We measured significant temperature-induced transmission losses in the samples having a polymide or aluminium coating and a thin cladding (1.1. or 1.2 cladding to core diameter ratio respectively). We observed negligible temperature-induced losses in fiber samples having a thick cladding (1.4 cladding to core diameter ratio). The losses increased with increasing wavelength and were very high in the infrared. The amount of losses depended also on the coating material. We attribute this phenomenon (also observed in the present study) to the dependence of microbending losses on temperature. The small diameter of the fiber coils greatly enhances this phenomenon.